

CHAPTER IV

**ISOTOPIC EXCHANGE:
CO₂ – O(¹D)**

4.1 INTRODUCTION

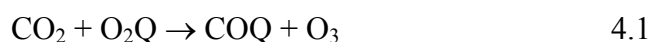
Ozone in the stratosphere is mass independently enriched in the heavy oxygen isotopes (¹⁷O and ¹⁸O) relative to the ambient oxygen from which it is formed (Krankowsky et al., 2000; Mauersberger et al., 2001). A detailed discussion about this mass independent enrichment is given in Chapter I of this thesis (§ 1.4). As ozone is a photochemically active species in the atmosphere, its mass independent signature can be transferred to other oxygen-containing molecules in the atmosphere (e.g. CO₂, N₂O, CO, H₂O etc.). The present chapter deals with the mechanism involved in the isotopic exchange between CO₂ and ozone through a ozone dissociation product, O(¹D).

4.1.1 Anomalous Oxygen Isotopic Composition of Stratospheric CO₂

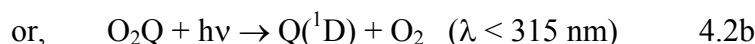
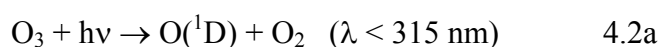
Isotopic measurements of stratospheric CO₂ clearly show that it is enriched in heavy oxygen isotopes (Gamo et al., 1989, 1995; Thiemens et al., 1991, 1995) and this enrichment (both in ¹⁸O and ¹⁷O) increases with altitude (Lämmerzahl et al., 2002). Moreover, the enrichments in ¹⁷O and ¹⁸O are linearly related with slope 1.7 (Lämmerzahl et al., 2002). Following a different method, Bhattacharya et al. (Bhattacharya, S.K., R.J. Francey, C.E. Allison, I. Levin, U. Schmidt, and T. Gamo, Altitudinal variation in oxygen isotopic composition of the stratospheric carbon dioxide, paper under preparation for *J. Geophys. Res.*) also obtained a slope much higher than unity and showed that depending upon the sampling altitude it varies from 1.2 to 2.2. Further discussion about oxygen isotopic composition of stratospheric CO₂ is presented in Chapter V (§ 5.3).

4.1.2 Mechanism of the Isotopic Exchange Between CO₂ and O(¹D)

Yung et al. (1991) and Thiemens et al. (1991) proposed that stratospheric ozone is the real source of “heaviness” of the stratospheric CO₂. The direct transfer of “heaviness” from the ozone pool to the CO₂ pool by the reaction,



where Q is the heavy oxygen isotopic species: ¹⁷O or ¹⁸O, is quite inefficient. Yung et al. (1991) proposed the transfer mechanism via O(¹D), a very reactive species, produced during UV photolysis of O₃. The reaction schemes are as follows,



The quenching rate of O(¹D) by CO₂ is quite high (DeMore et al., 1997). The quenching rate coefficient at T = 298 K is $\sim 1.1 \times 10^{-10} \text{ cm}^3 \text{ s}^{-1}$ (the same for Ar and Kr are 7×10^{-13} and $8 \times 10^{-12} \text{ cm}^3 \text{ s}^{-1}$ respectively). The high efficiency of the CO₂ + O(¹D) quenching is somewhat unusual given the fact that it is spin forbidden. So, the quenching mechanism is thought to be through an intermediate CO₃^{*} as follows:

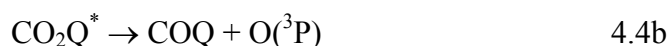
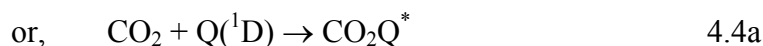


Table 4.1. List of essential reactions involved in the mechanism of “heavy” isotope transfer from O₃ pool to CO₂ pool along with their reaction coefficients. The molecular kinetic data are taken from DeMore et al. (1997).

Reaction Pathway	Photo-dissociation Coefficients (s ⁻¹)
O ₃ + hv → O(¹ D) + O ₂ (λ < 315 nm)	J ₁ = 7.4 × 10 ⁻⁵
O ₂ Q + hv → Q(¹ D) + O ₂ (λ < 315 nm)	J ₂ = ½ J ₁ = 3.7 × 10 ⁻⁵
	Rate Constant (cm ³ s ⁻¹)
O(¹ D) + CO ₂ → CO ₂ + O(³ P)	k ₁ = 7.4 × 10 ⁻¹¹ e ^{120/T}
Q(¹ D) + CO ₂ → COQ + O(³ P)	k ₂ = 2/3 k ₁ = 4.9 × 10 ⁻¹¹ e ^{120/T}
O(¹ D) + COQ → CO ₂ + Q(³ P)	k ₃ = 1/3 k ₁ = 7.4 × 10 ⁻¹¹ e ^{120/T}
O(¹ D) + O ₃ → O ₂ + O ₂	k ₄ = 1.2 × 10 ⁻¹⁰ e ^{80/T}
O(¹ D) + O ₂ → O ₂ + O(³ P)	k ₅ = 3.2 × 10 ⁻¹¹ e ^{67/T}
Q(¹ D) + O ₂ → O ₂ + Q(³ P)	k ₆ = k ₇ = 3.2 × 10 ⁻¹¹ e ^{67/T}
O + O ₃ → O ₂ + O ₂	k ₈ = 8.0 × 10 ⁻¹² e ^{70/T}

The existence of CO₃^{*} was first proposed by Katakis and Taube (1962). CO₃^{*} is a sufficiently long-lived species, with a life time of 10⁻¹¹ to 10⁻¹² seconds and it pre-dissociates to CO₂ + O(³P). Low-temperature experimental studies (Jacox and Milligan, 1971; Moll et al., 1966; Weissberger et al., 1967) and *ab initio* calculations (Froese and Goddard, 1993) indicate that CO₃^{*} intermediate has C_{2v} symmetry with the structure shown in Figure 4.1. The transfer of “heaviness” from the O₃ to the CO₂ pool can also be imagined through O(³P), an ozone photolysis product at visible wavelength. However, the

reactivity of this species is very low, and it was not considered effective for the isotopic transfer process. The reactions involved in the mechanism along with their rate coefficient are shown in Table 4.1.

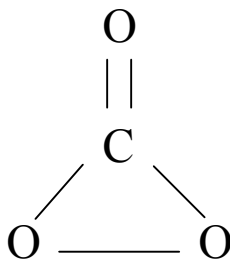


Figure 4.1. Structure of CO_3^* intermediate with C_{2v} symmetry (Froese and Goddard, 1993)

4.1.3 Previous Experimental Studies

So far, two experimental studies have been carried out (Wen and Thiemens, 1993; Johnston et al., 2000) to understand the isotopic exchange mechanism. In the first study, Wen and Thiemens (1993) photolyzed O_3 and CO_2 till most of the O_3 was decomposed to O_2 . They measured the isotopic composition of the final O_2 and inferred the composition of CO_2 assuming a mass balance. Based on these data they argued that the exchange does not occur through a simple statistical mixing between O-atom and CO_2 but involves a mass-independent fractionation presumably through CO_3^* . However, there were some limitations in the Wen and Thiemens (1993) experiments as far as application to stratosphere is concerned. The initial O_3 reservoir was not isotopically enriched and had a mass-dependent isotopic ratio contrary to what is observed in stratosphere. Also, the calculations were done assuming 100 % dissociation of O_3 , which was not strictly true (see Table 1 of their paper). Thus, even though their conclusions were correct one cannot use their data for quantitative derivation of $\delta^{17}\text{O} - \delta^{18}\text{O}$ slope in stratosphere.

In another set of experiments, Johnston et al., (2000) photolyzed O_2 and CO_2 of known isotopic composition with variable O_2/CO_2 reservoir ratio. They measured the two oxygen isotope ratios of the final CO_2 in cases where the CO_2/O_2 ratio was high (0.336 to 3.94). But they did not measure the $\delta^{17}\text{O}$ of CO_2 for those experiments where the ratio was low ($\sim 1/1000$) as in the case of atmosphere. Moreover, in their experiments there was no O_3 at the beginning; the O_3 concentration built up slowly with corresponding increase in the extent of exchange of $\text{O}(^1\text{D})$, derived from O_3 photolysis, with CO_2 . This

is unlike the case in stratosphere where there is always an ozone reservoir with enriched isotope ratios. Additionally, presence of oxygen reservoir introduces complications through its own quenching effect. Though the rate coefficient of quenching of $\text{O}(^1\text{D})$ with O_2 is 60 % of that with CO_2 , since the O_2 reservoir was quite large, the quenching of $\text{O}(^1\text{D})$ with O_2 became a major (unknown ?) factor in limiting the heavy oxygen isotope transfer to CO_2 . In view of these uncertainties, it is not clear why the “high- CO_2 ” experiments of Johnston et al. (2000) did not reproduce the observed stratospheric $\delta^{17}\text{O} - \delta^{18}\text{O}$ slope of more than one which prompted them to suggest that further experiments with “low- CO_2 ” are required to clarify the issue.

4.1.4 Numerical Model Studies

Two numerical model studies were carried by Yung et al. (1997) and Barth and Zahn (1997) to explain the laboratory data as well as stratospheric observations. Yung et al. (1997) applied a mixing model (first proposed by Yung et al., 1991) to explain the laboratory results of Wen and Thiemens (1993) following the chemical scheme given by the Equations 4.3 and 4.4. Yung et al. (1997) varied the isotopic composition of initial O_3 by 200 ‰ in their model and observed that at equilibrium the isotopic composition of O_2 reservoir varied only by 14 ‰. This insensitivity to the isotopic composition of the initial O_3 is attributed to the fact that the $\text{O}(^1\text{D})$, originating in O_3 photolysis, is quenched to $\text{O}(^3\text{P})$ during reaction with CO_2 . This $\text{O}(^3\text{P})$ can either then react with O_3 , forming two O_2 molecules, or it can combine with O_2 , reforming O_3 . Because the second reaction is orders of magnitude faster than the first, oxygen atoms cycle through O_3 many times before ending up as O_2 . Yung et al. (1997) argued that this “wash-out” effect, combined with the fact that the CO_2 reservoir is much larger than O_2 reservoir ($\text{CO}_2 : \text{O}_2 = 20 : 1$), can explain the laboratory results of Wen and Thiemens (1993). Whereas the model is able to reproduce the experimental ^{18}O results, it does not succeed in reproducing the ^{17}O results. Incorporating the same enrichment mechanism into a 1-D atmospheric model Yung et al. (1997) predict a ^{18}O enrichment profile in stratospheric CO_2 ; they found that, by doubling the eddy diffusion coefficient, the model predicted profile roughly matched the observations.

With different sets of assumptions Barth and Zahn (1997) tried to explain the laboratory data of Wen and Thiemens (1993) and the stratospheric data (Zipf and Erdman, 1994; Thiemens et al., 1995). As a first step, they constructed four different

vertical profiles (P1 to P4) of $\delta^{18}\text{O}$ of stratospheric ozone by using (i) the measured middle stratosphere profiles of Mauersberger (1981), (ii) setting the tropospheric value ($\delta^{18}\text{O} = 116 \text{ ‰}$) for the whole stratosphere, (iii) and (iv) using Irion et al. (1996) and Meier and Notholt (1996) data which show increasing $\delta^{18}\text{O}$ values in ozone above tropopause and reach a constant maximum value of $\delta^{18}\text{O} = 150$ and 160 ‰ respectively above 40 km. Since little was known about the $\delta^{17}\text{O}$ in ozone, they assumed a fixed offset of $\Delta = \delta^{18}\text{O} - \delta^{17}\text{O} = 34 \text{ ‰}$ using the tropospheric observations of Krankowsky et al. (1995). They justified this constant offset on the basis of laboratory data of Morton et al., 1990.

As the input of their model, they considered an enhanced isotopic composition of $\text{O}(^1\text{D})$ compared to O_3 since the isotopic composition of $\text{O}(^1\text{D})$ produced by O_3 photolysis should be modified by the mass dependent collision rates with N_2 and O_2 . They estimated 19 and 36 ‰ increase in $\delta^{17}\text{O}$ and $\delta^{18}\text{O}$ of $\text{O}(^1\text{D})$ compared to the O_3 composition for all the four profiles (P1 to P4).

They first run their model using the profiles P1 to P4 following the reaction scheme (given by Equations 4.3 and 4.4). While trying to match the measured altitudinal profile of $\delta^{18}\text{O}$ in CO_2 , they realized the necessity of introducing an extra fractionation process in the model. They postulated that the isotopic exchange between $\text{O}(^1\text{D})$ and CO_2 operates faster for ^{17}O than for ^{18}O resulting in a fractionation. This fractionation (ϵ) was incorporated as a mass dependent fractionation during the formation of CO_3^* . Using the P4 profile and assuming $\Delta = 34 \text{ ‰}$ and $\epsilon = (32 \pm 7)$ and $(64 \pm 14) \text{ ‰}$ for ^{17}O and ^{18}O respectively, they could reproduce the observations of Zipf and Erdman (1994) and Thiemens et al. (1995) for both $\delta^{18}\text{O}$ and $\delta^{17}\text{O}$ in stratospheric CO_2 .

4.1.5 Motivation Behind the Present Work

The two aspects (isotopic enrichment and slope) of stratospheric CO_2 (as described in § 4.1.1) pose interesting challenge to atmospheric scientists. The motivation of the present work was to further constrain the factors affecting the isotope transfer in stratospheric CO_2 and especially check if the observed high slopes (Lämmerzahl et al., 2002) could be obtained in the laboratory using O_3 and CO_2 of relevant stratospheric isotopic composition. An important question is whether the proposed mechanism has the potential for preferential transfer of ^{17}O relative to ^{18}O from the ozone pool to the CO_2 pool.

4.2 ABOUT THE EXPERIMENT

The presence of a large oxygen reservoir in the experiments of Johnston et al. (2000) complicates the issue of isotopic transfer between CO_2 and O_3 pools through quenching of $\text{O}(^1\text{D})$ by oxygen. Therefore, a simple experiment was designed to study oxygen isotope exchange process between CO_2 and $\text{O}(^1\text{D})$ (derived from UV photolysis of ozone). Photolysis of a mixture of CO_2 (of mass dependent composition) and O_3 (of mass independent composition) was carried out for various periods (< 30 minutes) using appropriate UV wavelengths. The present experimental conditions are obviously not similar to that of stratosphere since a large oxygen reservoir is missing, but it was felt that the mechanism involved in the isotope transfer between these two stratospheric oxygen bearing species (O_3 and CO_2) can be better understood if other interfering effects are absent.

Two different sets of experiments were performed. In set I, photolysis of ozone of fixed isotopic composition with CO_2 of three distinctly different oxygen isotopic composition (in three different sub-sets) was done and, in set II, photolysis of CO_2 of fixed isotopic composition with ozone of nine different isotopic compositions was done.

4.2.1 Preparation of O_3 of fixed isotopic composition

Ozone was produced in a 5-liter spherical chamber fitted with a MgF_2 window by irradiating ultra-pure oxygen ($\delta^{18}\text{O} = 24.6 \text{ ‰}$, $\delta^{17}\text{O} = 12.5 \text{ ‰}$ with respect to V-SMOW) at 500 torr pressure with UV generated by a Hg resonance lamp (184 and 254 nm) driven by a micro-wave generator as described in Chapter II (§ 2.2.2). Photolysis was carried out for about six hours (irradiation time was decided based upon the previous experiments described in Chapter II (§ 2.2.2)). After photolysis, the formed ozone was frozen by LN_2 and the oxygen pumped away till 2 mtorr pressure (vapor pressure of ozone at LN_2). A 1-liter flask was connected to the 5-liter chamber and the formed ozone was equilibrated within the total volume ($5 + 1 = 6$ liters). After equilibration, the 5-liter chamber was isolated and the ozone within the 1-liter flask was collected in a molecular sieve with LN_2 and converted to oxygen (as described in § 2.2.2). The mass-spectrometric measurement of this aliquot of oxygen provides the isotopic composition of the ozone as well as the estimate of the remaining amount (see § 2.2.2 for more details) within the 5-liter chamber. The irradiation protocol (6 hrs with input power of 80 watts and reflected power 10 watts) was strictly maintained to ensure retrieval of essentially the same amount of

ozone with nearly the same isotopic composition ($\sim 800 \mu\text{mole}$ with $\delta^{17}\text{O} = 110 \pm 4 \text{ ‰}$ and $\delta^{18}\text{O} = 124 \pm 2 \text{ ‰}$ wrt SMOW; the δ -values are always expressed wrt SMOW). Longer (~ 14 hrs) irradiation was done in two cases to get more amount of ($\sim 2000 \mu\text{mole}$) ozone, the time being decided based on the production rate of ozone at 500 torr of O₂ pressure ($2.5 \mu\text{mole per min}$) for the particular experimental set up (see Chapter II for details).

4.2.2 Preparation of CO₂ and O₃ of different isotopic compositions

Four different isotopic compositions of CO₂ were used in the whole experiment. The primary CO₂ was a tank CO₂ (99.99 % pure) from Vadilal Gas Company, Ahmedabad (India) with isotopic composition of $\delta^{18}\text{O} = 17.40 \text{ ‰}$ and $\delta^{17}\text{O} = 9.04 \text{ ‰}$. This CO₂ was equilibrated with water of three different isotopic compositions: a) V-SMOW water ($\delta^{18}\text{O} = 0.0 \text{ ‰}$ and $\delta^{17}\text{O} = 0.0 \text{ ‰}$), b) South-Pole water ($\delta^{18}\text{O} = -45 \text{ ‰}$ and $\delta^{17}\text{O} = -23.5 \text{ ‰}$) and, c) SLAP water ($\delta^{18}\text{O} = -55 \text{ ‰}$ and $\delta^{17}\text{O} = -28.5 \text{ ‰}$). In each of the three cases, $1200 \mu\text{mole}$ of CO₂ was equilibrated for 2 days with 4 cc of water. After 2 days, CO₂ was extracted and cleaned by the usual procedure (passing repeated number of times through -90°C slush). The three CO₂ gas samples made this way will be abbreviated as SM-CO₂, SP-CO₂ and SL-CO₂ respectively.

The strategy to produce ozone of different isotopic composition was based on the fact that UV dissociation of ozone (see Chapter III for more details) enriches the left-over ozone pool. The steps taken were as follows: the initial ozone was produced as described in the previous section (§ 4.2.1). This ozone was dissociated to the extent of 30 to 97 % by a Hg lamp and the left-over ozone was separated cryogenically from the product oxygen. The left-over ozone in the reaction chamber was treated as the initial ozone for the exchange with CO₂. The amount of ozone left in the chamber was, of course, not constant but decreased with increasing enrichment. The maximum enrichment observed was about 80 and 50 ‰ with respect to the initial ozone (124 and 110 ‰) in $\delta^{18}\text{O}$ and $\delta^{17}\text{O}$ respectively at the dissociation level of $\sim 97 \text{ ‰}$, which reduces the ozone reservoir to about $20 \mu\text{mole}$.

4.2.3 CO₂ – O(¹D) Isotopic Exchange

The isotopic exchange was carried out by photolysis of a CO₂ – O₃ mixture for a certain time. Two sets of experiments were performed. The first set of experiment

consisted of three subsets with ozone of fixed isotopic composition and CO₂ of three distinctly different compositions as follows: sub-set Ia: SM-CO₂ with $\delta^{17}\text{O} = 20.35 \text{ ‰}$ and $\delta^{18}\text{O} = 39.33 \text{ ‰}$, sub-set Ib: SP-CO₂ with $\delta^{17}\text{O} = 2.15 \text{ ‰}$ and $\delta^{18}\text{O} = 4.09 \text{ ‰}$, and sub-set Ic: SL-CO₂ with $\delta^{17}\text{O} = -5.55 \text{ ‰}$ and $\delta^{18}\text{O} = -0.91 \text{ ‰}$. In each case, 100 μmole of CO₂ was taken in the 5-liter chamber from the respective reservoirs and the same Hg lamp was used for photolysis of the mixture. The time of photolysis was varied (up to 25, 23 and 26 minutes for set Ia, Ib, and Ic respectively) to get a wide range of enrichment in CO₂.

In the second set of experiment, the amount (100 μmole) of CO₂ (called V-CO₂ hereafter) as well as its isotopic composition ($\delta^{18}\text{O} = 17.28 \text{ ‰}$ and $\delta^{17}\text{O} = 8.98 \text{ ‰}$) was kept constant. The isotopic composition of O₃ was varied by the process described in the previous section (§ 4.1.2) from 124 to 205.7 ‰ in $\delta^{18}\text{O}$. The corresponding change in the amount of O₃ was from 300 μmole to 30 μmole . Depending upon the initial O₃ amount, photolysis time (estimated beforehand) was varied in such a way that 80 to 90 % of O₃ dissociation occurs during the photolysis.

After photolysis of the CO₂ – O₃ mixture, the product O₂, final CO₂ and left-over O₃ were separated following the procedure of Johnston et al (2000). CO₂ and left-over O₃ were trapped at the bottom of the reaction chamber by LN₂ and the product oxygen was collected in a sample bottle with molecular sieve with LN₂. CO₂ – O₃ mixture was collected in a 50 cc bottle (containing nickel flakes, properly degassed beforehand at $\sim 200^\circ \text{C}$) with LN₂. After the total transfer, the nickel-containing bottle was closed and it was heated up mildly for about 20 minutes. Mild heating in the presence of Nickel decomposes O₃ to O₂ (Johnston et al., 2000). After 20 minutes, CO₂ and O₂ (from decomposed O₃) were collected cryogenically one after another.

4.2.4 Isotopic Measurement of Oxygen and CO₂

The isotopic measurements were done in GEO 20-20 (Europa Scientific) mass-spectrometer. For oxygen isotopic measurement, the sample bottle used to collect oxygen and ozone (converted to oxygen) samples were of 1 cc with few pellets of molecular sieve in it. The major beam (mass 32) was calibrated beforehand with different amounts of oxygen samples using the same sample bottles. The calibration was used to estimate the amount of sample (as described in § 2.2.2). The estimated uncertainty in δ -values is 0.1 ‰ for $\delta^{18}\text{O}$ and 0.2 ‰ for $\delta^{17}\text{O}$ based on a few repeat measurements.

The oxygen isotopic ($\delta^{18}\text{O}$ and $\delta^{17}\text{O}$) measurements of CO₂ are not straight forward due to the fact that the isotopomers with mass 45 represents $^{16}\text{O}^{13}\text{C}^{16}\text{O}$ as well as $^{17}\text{O}^{12}\text{C}^{16}\text{O}$. The $\delta^{17}\text{O}$ and $\delta^{18}\text{O}$ of the final CO₂ were determined using the value of $\delta^{45}\text{R}$ and $\delta^{46}\text{R}$ and assuming invariance of $\delta^{13}\text{C}$ before and after the photolysis since there is no loss or gain of carbon in the exchange process (Johnston et al., 2000). The measured ratios of the CO₂ isotopomers can be expressed in terms of the individual oxygen and carbon isotopic ratios as follows:

$$\begin{aligned} \text{R}^{45} &= (\text{molecules with mass 45})/(\text{molecules with mass 44}) \\ &= ([^{16}\text{O}^{13}\text{C}^{16}\text{O}] + [^{16}\text{O}^{12}\text{C}^{17}\text{O}] + [^{17}\text{O}^{12}\text{C}^{16}\text{O}]) / [^{16}\text{O}^{12}\text{C}^{16}\text{O}] \\ &= \text{R}^{13} + 2(\text{R}^{17}) \end{aligned} \quad (4.5)$$

and, $\text{R}^{46} = (\text{molecules with mass 46})/(\text{molecules with mass 44})$

$$\begin{aligned} &= ([^{16}\text{O}^{12}\text{C}^{18}\text{O}] + [^{18}\text{O}^{12}\text{C}^{16}\text{O}] + [^{16}\text{O}^{13}\text{C}^{17}\text{O}] + [^{17}\text{O}^{13}\text{C}^{16}\text{O}] + [^{17}\text{O}^{12}\text{C}^{17}\text{O}]) / \\ & \quad [^{16}\text{O}^{12}\text{C}^{16}\text{O}] \\ &= 2(\text{R}^{18}) + 2(\text{R}^{13}\text{R}^{17}) + (\text{R}^{17})^2 \approx 2(\text{R}^{18}) \end{aligned} \quad (4.6)$$

(Note the symmetry factor 2 to convert atomic ratios to the molecular ratios)

so, $\delta_{std}^{45}X = (\text{R}^{45X} / \text{R}^{45std} - 1) \times 10^3 = \{[(\text{R}^{13} + 2\text{R}^{17})^X / (\text{R}^{13} + 2\text{R}^{17})^{std}] - 1\} \times 10^3$ (4.7)

and, $\delta_{std}^{46}X = (\text{R}^{46X} / \text{R}^{46std} - 1) \times 10^3 = \{[(2\text{R}^{18})^X / (2\text{R}^{18})^{std}] - 1\} \times 10^3$ (4.8)

By simple algebra,

$$\delta_{std}^{13}X = (1 + 2Z) \delta_{std}^{45}X + 2Z \delta_{std}^{17}X \quad (4.9)$$

where, $Z = (\text{R}^{17}/\text{R}^{13})^{std} = 15.38315937$ [for our tank CO₂, the mass-spectrometer standard]

and, $\delta_{std}^{18}X = \delta_{std}^{46}X$ (4.10)

In the course of oxygen isotopic measurements in CO₂, δ_{std}^{45} and δ_{std}^{46} were measured and using equations (4.9) and (4.10) and considering no change in ^{13}R in the process, $\delta^{17}\text{O}$ and $\delta^{18}\text{O}$ of the sample CO₂ were calculated.

For some cases, the isotopic ratios of all the three final products were measured to ensure the validity of the O-isotope mass balance. Considering transfers of gases, taking of aliquots, and several freezing and thawing the uncertainty in δ -values are little higher than that of direct oxygen measurements; we estimate an overall uncertainty of 0.2 ‰ for $\delta^{18}\text{O}$ and 0.5 ‰ for $\delta^{17}\text{O}$ for the final data based on a few repeat measurements.

4.2.5 Test of Recovery Yield of CO₂ and Blank $\delta^{13}\text{C}$

In view of the difficulties experienced by Johnston et al. (2000) in getting proper CO₂ yield in their “low-CO₂” experiments; great care was taken to perform these experiments. All stopcocks were of “Viton” O-ring type and no grease was used. Three blank experiments were done where CO₂ and O₃ were mixed and separated after keeping for an hour without photolysis. The isotopic composition of this CO₂ (treated as blank) was determined and shown in Table 4.2.

Table 4.2. δ^{45} and δ^{46} of V-CO₂ and CO₂ from three blank experiments when V-CO₂ was mixed with ozone of enriched oxygen isotopic composition and separated without photolysis (see text for details). The analysis is done w.r.t. a machine CO₂ reference having $\delta^{17}\text{O} = 9.04 \text{ ‰}$ and $\delta^{18}\text{O} = 17.40 \text{ ‰}$ with respect to SMOW. The δ -value differences between the mean of the blanks values and V-CO₂ (i.e., $\Delta\delta^{45} = 0.122 \text{ ‰}$ and $\Delta\delta^{46} = 0.410 \text{ ‰}$) are added with all δ^{45} and δ^{46} measurements as blank corrections.

CO ₂ Samples	δ^{45}	δ^{46}
V-CO ₂	-0.037	-0.119
Blank-1	-0.138	-0.732
Blank-2	-0.113	-0.405
Blank-3	-0.226	-0.450
Mean	-0.159	-0.530
δ -difference	-0.122	-0.41

The blank data show that there is slight decrease in δ -values of CO₂ due to mixing with O₃ and subsequent cryogenic separation. This decrease does not show up in the yield value, which was always close to 100 % (within 1 to 2 % which is the estimated experimental uncertainty in the yield measurement from mass-44 beam current). A small positive correction was applied to the measured δ^{45} and δ^{46} based on the mean blank values, i.e., $\delta^{45} = 0.12$ and $\delta^{46} = 0.41$. These corrections are well within the experimental uncertainties in the δ -values of CO₂.

4.3 RESULTS

The results of the photolysis experiments pertaining to sets Ia, Ib and Ic are given in Table 4.3 and show that the final CO₂ is enriched in both ¹⁷O and ¹⁸O in all the cases

and the enrichments increase with time of exposure. However, when the time is very large so that there is significant recycling of ozone the enrichment attains nearly steady value (see last two entries in set I, Table 4.3), which is reflected by the comparatively lower values of increase in ^{18}O enrichment. We did not investigate whether in each individual set the steady state was achieved or not since our objective was to check the slope value and this was nearly independent of the photolysis time for a given set of CO_2 and O_3 . Johnston et al. (2000) also found that the slope does not change even though the enrichment initially increases with time. The maximum ^{18}O -enrichments obtained are 11.4, 20.6 and 22.2 ‰ respectively for the three sets of experiments whereas the respective enrichments in ^{17}O are 19.3, 29.5 and 27.3 ‰. It is interesting to note that the enrichment in ^{17}O is always more than that in ^{18}O and this is clearly reflected in a plot of $\delta^{17}\text{O}$ vs. $\delta^{18}\text{O}$ (Figure 4.2).

In these experiments the isotopic composition of ozone is always kept constant (at $\delta^{17}\text{O} = 110.4$ and $\delta^{18}\text{O} = 124.9$ ‰) near the value observed in the stratosphere at the altitude of about 32 km (Mauersberger et al., 2001) (note that the values reported by Mauersberger et al., 2001 are with respect to atmospheric oxygen and the values reported here are with respect to SMOW). It is also seen that the slope relating $\Delta\delta^{17}\text{O}$ and $\Delta\delta^{18}\text{O}$ of the final CO_2 changes depending on the initial composition of CO_2 . Slope values of 1.29 ± 0.04 , 1.52 ± 0.04 and 1.81 ± 0.06 are obtained for composition of SL- CO_2 (-5.55, -10.91), SP- CO_2 (2.15, 4.09) and SM- CO_2 (20.35, 39.33), respectively i.e. the slope increases as the δ -values of the initial CO_2 increase and get closer to that of the ozone. Interestingly, the slope obtained from set Ia (with SM- CO_2 of tropospheric composition) experiment is close to the observed stratospheric slope 1.71 (Lämmerzahl et al., 2002).

The results for the set II experiments are given in Table 4.4. They show that the isotopic composition of final CO_2 depends on the initial ozone composition; higher the enriched in the initial ozone, more is the enrichment in the final CO_2 (keeping the photolysis time constant at around 3 minutes). The initial ozone composition varied from 124.9 to 205.7 ‰ for $\delta^{18}\text{O}$ and from 110.4 to 159.4 ‰ for $\delta^{17}\text{O}$. The two variations are related by a slope value of nearly 0.6. It is quite expected since the dissociation process results in such a slope for the left-over ozone (see chapter III; Chakraborty and Bhattacharya, 2002). On the other hand, this change in initial ozone composition results in a change of 9.8 ‰ in $\delta^{18}\text{O}$ and 18.5 ‰ in $\delta^{17}\text{O}$ of final CO_2 . The isotopic composition

of final CO_2 shows a linear trend of increase with a slope ($\Delta\delta^{17}\text{O}/\Delta\delta^{18}\text{O}$) of 1.94 as shown in Figure 4.3.

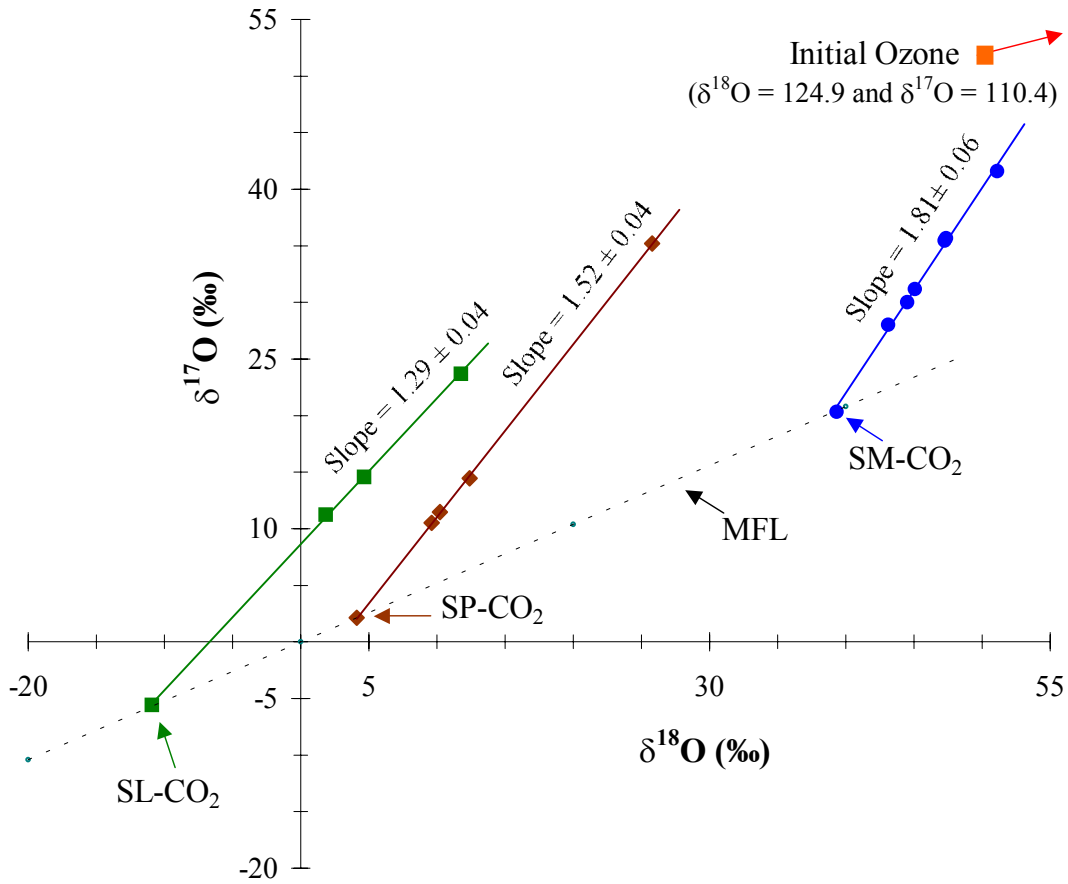


Figure 4.2. The $\delta^{17}\text{O}$ - $\delta^{18}\text{O}$ plot showing the evolution of isotopic composition of CO_2 as a result of exchange with $\text{O}(^1\text{D})$ derived from isotopically enriched ozone under UV exposure (initial compositions of both the gases are shown). With the increase in photolysis time the CO_2 gets more and more enriched in heavy isotope ratios but the change is higher in $^{17}\text{O}/^{16}\text{O}$ compared to $^{18}\text{O}/^{16}\text{O}$. The three different CO_2 gases (SM- CO_2 , SP- CO_2 and SL- CO_2 corresponding to set Ia, Ib and Ic respectively) evolve along three enrichment lines with slopes 1.81 ± 0.06 , 1.52 ± 0.04 and 1.29 ± 0.04 respectively. The slope for SM- CO_2 (similar in composition to tropospheric CO_2) is close to the one (1.71) observed in stratosphere. The line labeled as MFL denotes the terrestrial mass fractionation line (slope 0.5). The error of each data point is comparable to its size.

Table 4.3. Oxygen isotopic composition of CO₂ after exchange with O(¹D) derived from UV photolysis of isotopically enriched O₃ in the set Ia, Ib and Ic experiments using three different initial CO₂ (SM-CO₂, SP-CO₂ and SL-CO₂) but same composition of O₃. The amount of O₃ and CO₂ were 800 and 100 μmole respectively except in two cases as shown. The CO₂ gets enriched after exchange with slopes relating the two isotopic enrichments higher than one (see text). Set Ia yields slope value of 1.81 ± 0.06 (obtained from Figure 1), which is similar to that found in stratosphere.

Set No.	Initial CO ₂		Initial O ₃ ^{***}		Amount of CO ₂ (μmole)	Amount of O ₃ (μmole)	Photolysis Time (t- min)	Final CO ₂ ^{##}		Enrichment in CO ₂		Slope ^{**} (Δδ ¹⁷ O/Δδ ¹⁸ O)	Rate of Increase in ¹⁸ O Enrichment (Δ ¹⁸ O/t ‰/min)
	δ ¹⁷ O (‰)	δ ¹⁸ O (‰)	δ ¹⁷ O (‰)	δ ¹⁸ O (‰)				δ ¹⁷ O (‰)	δ ¹⁸ O (‰)	Δδ ¹⁷ O (‰)	Δδ ¹⁸ O (‰)		
Ia (SM-CO ₂)	20.35	39.33	110.4	124.9	100	800	9	28.0	42.7	7.6	3.8	1.90	0.42
					100	800	12	31.2	44.8	10.8	5.8	1.86	0.48
					100	800	15	35.5	46.8	15.1	8.0	1.83	0.53
					100	800	25	41.6	50.7	21.2	11.8	1.79	0.47
					(180) [•]	800	130	30.0	44.1	9.6	5.2	1.83	(0.04) [#]
				100	800	360	35.7	46.9	15.3	8.1	1.85	(0.02) [#]	
Ib (SP-CO ₂)	2.15	4.09	110.4	124.9	100	800	6	10.5	9.6	8.4	5.5	1.52	0.92
						800	7	11.5	10.2	9.3	6.1	1.52	1.33
						800	10	14.5	12.4	12.3	8.3	1.48	1.23
						(2000) [*]	23	35.2	25.8	33.1	21.7	1.52	0.94
Ic (SL-CO ₂)	-5.55	-10.91	110.4	124.9	100	800	13	11.3	1.8	16.8	12.7	1.32	0.97
						800	20	14.6	4.6	20.2	15.6	1.30	0.78
						(2000) [*]	26	23.7	11.7	29.3	22.7	1.29	0.87

^{***} The estimated uncertainty in δ-values of ozone is 0.2 ‰ for δ¹⁸O and 0.5 ‰ for δ¹⁷O based on few repeat measurements.

^{##} The estimated errors of oxygen isotopic measurement in final CO₂ are 0.5 and 1.0 ‰ in δ¹⁸O and δ¹⁷O respectively.

^{**} After propagation of error, the uncertainty in individual slope value is less than 10 %.

[•] In this case the initial amount of CO₂ was higher.

[#] In these cases the time was very large allowing for significant recycling of ozone.

^{*} In these cases the initial amount of ozone was higher.

Table 4.4. Experimental results for the exchange reactions between CO₂ and O₃ for the set II experiments. The CO₂ isotopic composition (V-CO₂) was kept constant whereas the isotopic composition of ozone was varied. The amount of CO₂ used for all the experiments was 100 μmole. The amount of ozone was not constant throughout but varied from 300 to 30 μmole depending upon its composition (higher the enrichment lower was the amount). All the oxygen isotopic data are expressed with respect to SMOW.

Initial CO ₂		Initial Ozone ^{**}		Photolysis Time (min)	Product Oxygen ^{**}		Left-over Ozone ^{**}		Final CO ₂ [#]	
δ ¹⁷ O (‰)	δ ¹⁸ O (‰)	δ ¹⁷ O (‰)	δ ¹⁸ O (‰)		δ ¹⁷ O (‰)	δ ¹⁸ O (‰)	δ ¹⁷ O (‰)	δ ¹⁸ O (‰)	δ ¹⁷ O (‰)	δ ¹⁸ O (‰)
8.98	17.28	110.4	124.9	3.0	92.0	109.0	118.0	137.1	18.3	21.4
8.98	17.28	112.2	131.5	3.5	102.7	118.4	125.4	152.8	21.2	22.4
8.98	17.28	109.5	132.2	3.5	101.4	118.3	120.1	149.3	32.8	29.1
8.98	17.28	117.7	141.0	4.0	108.9	128.2	128.1	158.4	33.8	29.4
8.98	17.28	119.4	142.0	3.0	107.2	125.9	128.1	156.0	26.8	25.0
8.98	17.28	123.7	150.3	3.5	114.0	136.3	134.5	167.2	24.2	24.0
8.98	17.28	128.8	156.5	3.5	118.7	141.6	138.1	172.5	23.8	23.4
8.98	17.28	145.5	184.5	2.3	127.4	154.0	142.5	177.0	26.2	25.5
8.98	17.28	159.4	205.7	2.5	138.7	166.7	NM [*]	NM [*]	36.8	31.2

^{**} The estimated uncertainty in δ-values of ozone (measured as oxygen) is 0.2 ‰ for δ¹⁸O and 0.5 ‰ for δ¹⁷O based on few repeat measurements.

[#] The estimated errors of oxygen isotopic measurement in final CO₂ are 0.5 and 1.0 ‰ in δ¹⁸O and δ¹⁷O respectively.

^{*} NM denotes not measured. As the amount was negligible it was not possible to measure the amount as well as the isotopic composition of the left-over ozone for that particular experiment.

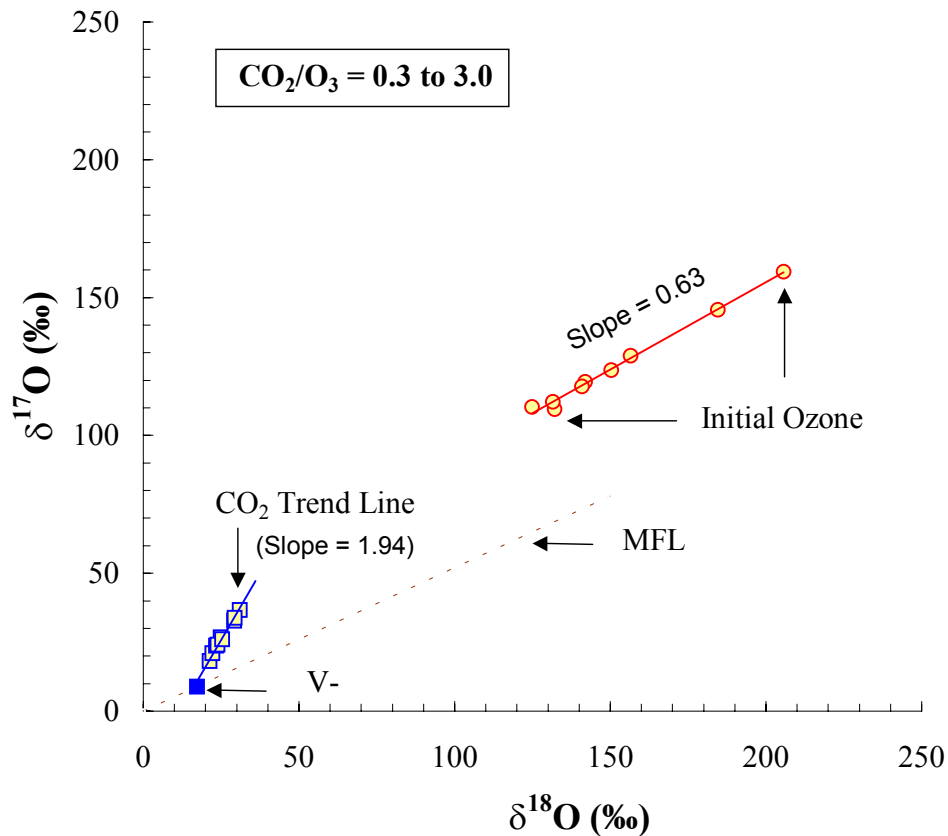


Figure 4.3. A three-isotope plot showing changes in δ -values of a fixed CO_2 ($V\text{-CO}_2$) as a result of exchange with $\text{O}(^1\text{D})$ derived from ozone of different initial compositions. As the isotopic composition of initial ozone increases, the enrichment in corresponding final CO_2 also increases. The different ozone samples were taken in such a way that they lie along a line of slope 0.63 close to the value in ozone samples from various stratospheric levels. The corresponding CO_2 points lie along a line of slope 1.94 which closely resembles the slope 1.71 found in CO_2 samples obtained from various stratospheric levels. The line labeled as MFL denotes the terrestrial mass fractionation line (slope 0.52). The error of each data point is comparable to its size.

4.4 DISCUSSION

According to the proposed (Yung et al., 1991) pathway of isotopic transfer from the ozone pool to the CO_2 pool, the exchange takes place through $\text{O}(^1\text{D})$, a UV dissociation product of O_3 . Therefore, to gain insight in the process, it is essential to estimate the isotopic composition of $\text{O}(^1\text{D})$.

4.4.1 Isotopic Composition of $\text{O}(^1\text{D})$

The isotopic composition of $\text{O}(^1\text{D})$ is derived based on the assumption that only terminal atoms in the ozone molecule can be broken to form $\text{O}(^1\text{D})$ during photo-dissociation of ozone. If ozone is isotopically enriched and the enrichment is mainly due

to concentration of the heavy isotope in the asymmetric species it is apparent that the O(¹D) reservoir would have enrichment higher than that of progenitor ozone since asymmetry is caused by placement of a heavy isotope in the terminal position. The derivation of the isotopic composition of O(¹D) follows closely the steps outlined by Janssen et al. (2001) to calculate the enrichment in ⁵⁰O₃ and is given in Chapter V (§ 5.4.1). Following the definition of enrichment, $E (\text{‰}) = [(\text{M}^{17}\text{O}_3 / \text{M}^{18}\text{O}_3)_{\text{measured}} / (\text{M}^{17}\text{O}_3 / \text{M}^{18}\text{O}_3)_{\text{calculated}} - 1] \times 1000 \text{ ‰}$, and the rate constants of different ozone forming channels, the isotopic composition of the asymmetric ozone is calculated and we assume that the O(¹D) has the same composition as that of the asymmetric ozone.

It is seen that under the terminal atom source assumption O(¹D) has an enriched composition ($\delta^{17}\text{O} = 150 \text{ ‰}$ and $\delta^{18}\text{O} = 150 \text{ ‰}$) relative to total initial oxygen (see Chapter V, § 5.4.1). For our experiment, the oxygen has the composition of $\delta^{17}\text{O} = 12.48 \text{ ‰}$ and $\delta^{18}\text{O} = 24.58 \text{ ‰}$ with respect to SMOW. Therefore, O(¹D) will have the composition, $\delta^{17}\text{O} = 164.1 \text{ ‰}$ and $\delta^{18}\text{O} = 178.3 \text{ ‰}$ with respect to SMOW.

It is logical to assume that this transient reservoir of O(¹D) is further modified by mass dependent collision rate of O(¹D) atoms with CO₂ molecules. In a simple collision model the rate coefficient for a chemical reaction is inversely proportional to $\sqrt{\mu}$ (where μ is the reduced mass). For simplicity we can think of this as a combination of two effects arising from two types of collisions: (i) collision between dominant CO₂ species (¹⁶O¹²C¹⁶O) and ¹⁶O, ¹⁷O and ¹⁸O isotopes and (ii) collision of ¹⁶O atoms with CO₂ species of mass 44, 45 and 46. The first type would yield a modified O(¹D) composition which is effective in collision with CO₂ while the second type would yield a modified CO₂ composition which is effective during collision with O(¹D).

Following this argument, the calculated reaction rate ratios between the colliding pairs CO₂ – ¹⁶O(¹D) and CO₂ – ¹⁷O(¹D) and CO₂ – ¹⁸O(¹D) are 0.977 and 0.957 respectively. Therefore, the effective O(¹D) composition would be $\delta^{17}\text{O} = 138.1 \text{ ‰}$ and $\delta^{18}\text{O} = 127.6 \text{ ‰}$ with respect to SMOW. Similarly, the CO₂ composition will get modified by the factors 0.997 and 0.994 for ⁴⁵R and ⁴⁶R respectively.

4.4.2 Failure of Two-Component Mixing

A simple mixing of modified SM-CO₂ ($\delta^{17}\text{O} = 17.32 \text{ ‰}$ and $\delta^{18}\text{O} = 33.29 \text{ ‰}$) and modified O(¹D) composition ($\delta^{17}\text{O} = 138.1 \text{ ‰}$ and $\delta^{18}\text{O} = 127.6 \text{ ‰}$) representing the end members of set Ia experiment would result in slope value of 1.28 in the scrambled CO₃*

(Figure 4.4). During formation of CO_2 and O-atom from CO_3^* , a mass dependent fractionation with lighter O-atom is expected. Therefore, the oxygen isotopic composition of the product CO_2 would lie over the secondary fractionation line (shown by the line BC in Figure 4.4) and hence, the slope value of the final CO_2 would be lower than 1.28 (the value for the scrambled CO_3^*). This limit of the slope value of 1.28 is drastically different from what is observed in set Ia experiment (1.81, Figure 4.2). A similar mixing calculation yields slopes of 1.07 and 1.02 for modified CO_2 compositions of set Ib ($\delta^{17}\text{O} = -0.62 \text{ ‰}$ and $\delta^{18}\text{O} = -1.75 \text{ ‰}$) and set Ic ($\delta^{17}\text{O} = -8.50 \text{ ‰}$ and $\delta^{18}\text{O} = -16.66 \text{ ‰}$) experiments. The corresponding observed slopes for set Ib and set Ic experiments are 1.52 and 1.29 clearly demonstrating preferential transfer of ^{17}O (relative to ^{18}O) to the CO_2 pool. It is also interesting to note that the value of the slope (1.81) obtained for typical stratospheric O_3 and CO_2 composition (set Ia) agrees well with the observed value (1.71) of Lämmerzahl et al. (2002). This agreement between the observed and experimental slopes is not accidental. The two end-member (CO_2 and $\text{O}(^1\text{D})$) compositions along with the applicable fractionation related to isotopic transfer decides the slope of the final CO_2 evolution line. In the stratosphere, the CO_2 concentration is much higher than O_3 concentration and the interaction time is not only longer (year scale) but also cumulative as the CO_2 ascends upwards. Consequently, the isotopic enrichment increases continuously with altitude due to increase in the time of interaction. A similar effect of enrichment increase with irradiation time is seen in the present laboratory experiment.

A major difference between the stratosphere and the present laboratory condition is the possibility of additional quenching of $\text{O}(^1\text{D})$ in stratosphere by other major species like N_2 and O_2 . This quenching would diminish the available $\text{O}(^1\text{D})$ reservoir and consequently the isotopic enrichment imparted to CO_2 . However, this large magnitude of quenching in stratosphere is compensated by long interaction time (a few years) between CO_2 and ozone-derived $\text{O}(^1\text{D})$ which makes it possible to achieve large isotopic enrichment in CO_2 from a rather small reservoir of ozone. On the other hand, reasonable enrichment in CO_2 could be attained in the laboratory in short time by having much larger amount of highly enriched ozone.

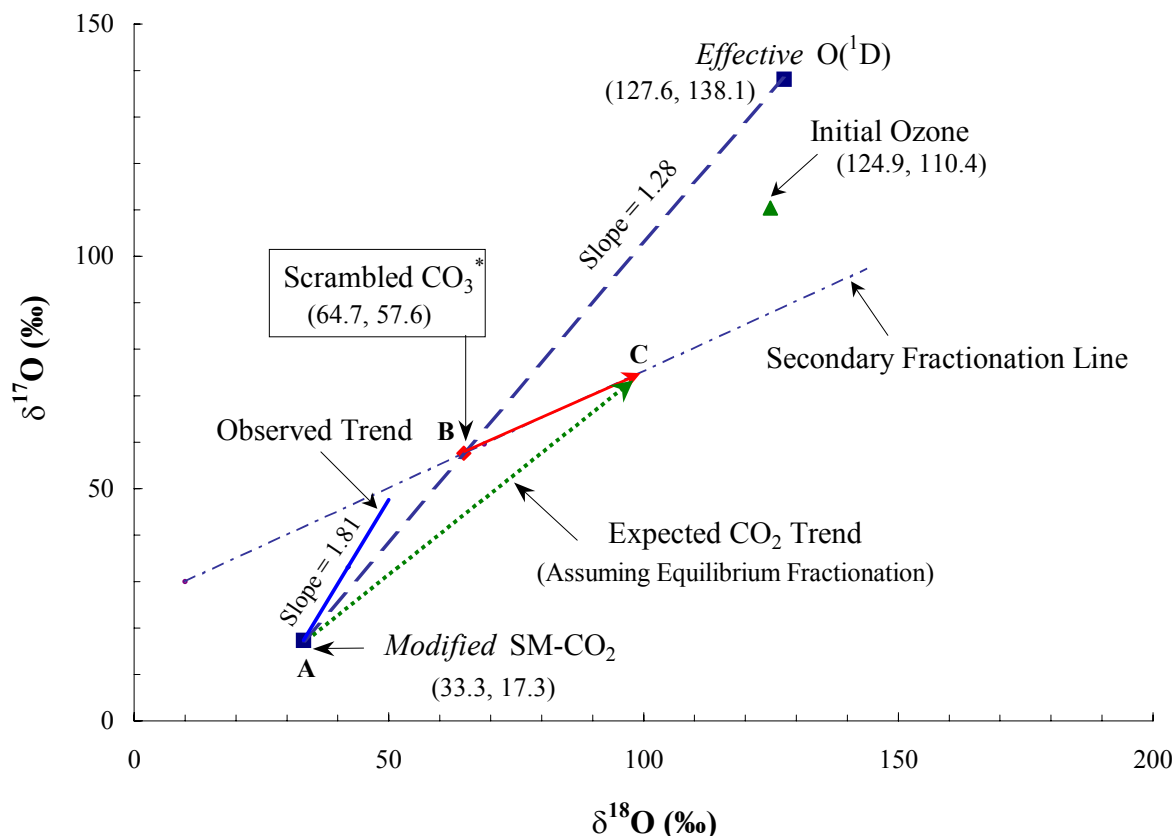


Figure 4.4. Schematic representation of two component mixing (for set Ia) using the effective $\text{O}(^1\text{D})$ composition as one end member and modified SM- CO_2 composition (point A) as other end member. B represents the composition of CO_3^* obtained by simple mixing of these two components. The slope of this mixing line (represented by AB) is 1.28. During the breakdown of CO_3^* product CO_2 is expected to incorporate the heavy isotopes preferentially and fractionate along the secondary fractionation line. C represents one such final CO_2 composition (assuming equilibrium fractionation) and AC represents the corresponding CO_2 evolution trend with a slope less than that of the simple mixing line AB i.e., 1.28. In contrast, the observed trend is 1.81 demonstrating ^{17}O preference to CO_2 in such exchange process.

4.4.3 Previous Results in the Light of Present Experiment

A re-plot (Figure 4.5) of Wen and Thiemens (1993) data of final CO_2 compositions (see Table 1 of their paper) along with their initial CO_2 and O_3 compositions in the same format as in Figure 1 shows that the final CO_2 evolves along a line with a slope value of 0.97 during isotopic exchange. They used ozone and CO_2 of mass dependent composition and it can be assumed that the derived $\text{O}(^1\text{D})$ from O_3 photolysis would be of the same composition as that of ozone (since the isotopic distribution within ozone molecule would be statistical in this case). Since the modification of the compositions of the two reservoirs due to collisional effect is mass

dependent, the effective $\text{O}(^1\text{D})$ ($\delta^{17}\text{O} = -1.37\text{‰}$ and $\delta^{18}\text{O} = -3.47\text{‰}$) as well as the modified CO_2 ($\delta^{17}\text{O} = 0.107\text{‰}$ and $\delta^{18}\text{O} = -0.76\text{‰}$) compositions would essentially lie over the mass fractionation line with a slope value of 0.52 (the modified $\text{O}(^1\text{D})$ and CO_2 compositions are calculated following the arguments of § 4.4.1). A simple mixing calculation (similar to that described for the present study in § 4.4.2), using these two end-member compositions, i.e., effective $\text{O}(^1\text{D})$ and initial CO_2 yields the same slope as that of mass fractionation line for the scrambled CO_3^* . Since the second stage of fractionation during separation of CO_3^* to form CO_2 is also mass dependent, the composition of final CO_2 would essentially lie over the same mass fractionation line. Therefore, this analysis reflects preferential transfer of ^{17}O to the CO_2 pool in Wen and Thiemens' experiment as observed in the present experiments.

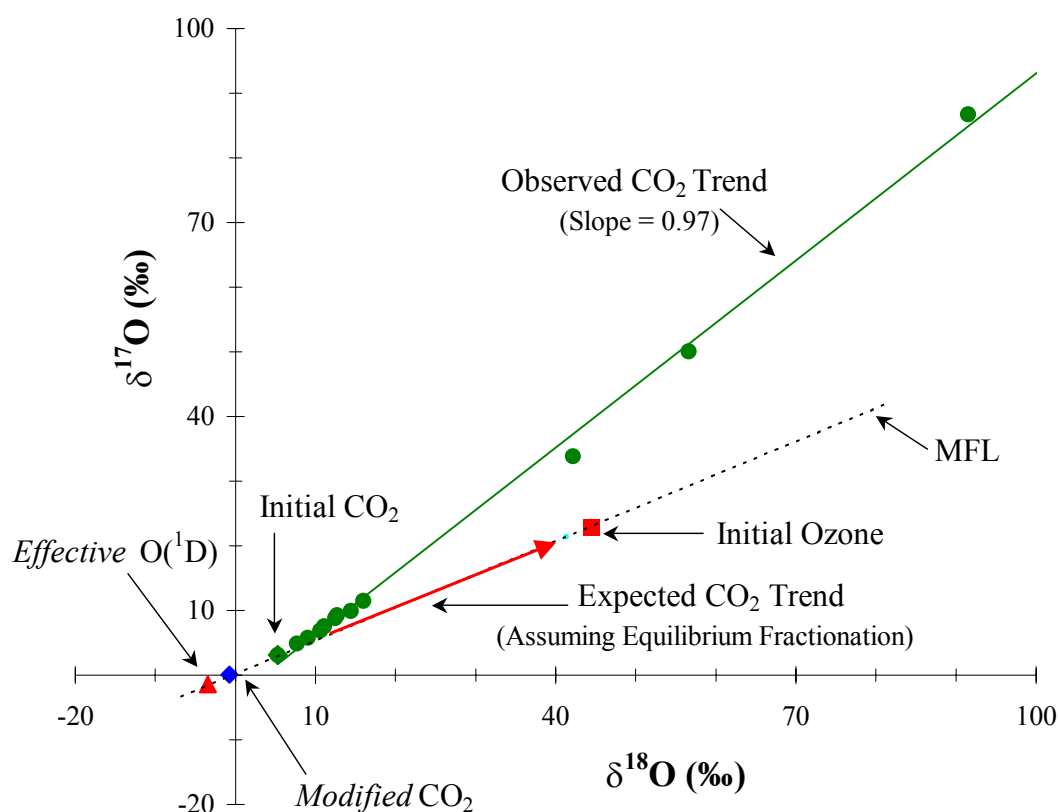


Figure 4.5. Three-isotope plot of the data from the experiment of Wen and Thiemens (1993) showing the compositions of initial CO_2 and O_3 and the progression of final CO_2 compositions (data taken from their Table 1 expressed with respect to SMOW) as a result of photolysis of $\text{CO}_2 - \text{O}_3$ mixture. The photolysis was done till O_3 was completely decomposed to O_2 . The expected slope based on similar considerations as in Figure 4.4 is 0.52 (i.e. mass-dependent) in contrast to the observed slope of 0.97 again indicating preferential ^{17}O transfer in exchange of CO_2 with $\text{O}(^1\text{D})$.

For long UV exposure, Wen and Thiemens (1993) observed negligible change in the composition of product oxygen even with large variation in the initial ozone composition. This phenomenon was interpreted as a “wash-out” effect by Yung et al. (1997) signifying numerous recycling of oxygen atoms through ozone and oxygen molecular reservoirs in the presence of a large CO_2 reservoir, which destroys the isotopic signature of the original O_3 . In contrary, no such situation arises in the present experiment since the recycled ozone component is negligible. The recycle ozone component is estimated from the experimental results of Chapter II (§ 2.4.7), which shows that at the most 0.2 μmole of ozone can be regenerated from product oxygen photolysis due to short photolysis time (~ 25 minutes) (also see Bhattacharya et al., 2002).

4.4.4 Supportive Evidence for Preferential ^{17}O Transfer

Another way to look at the results of the present study is to plot the compositions of the left-over ozone and product oxygen along with initial and final CO_2 compositions (Figure 4.6). The left-over ozone and the product oxygen follow two different slopes having values of 0.63 and 0.98 respectively (with respect to initial ozone composition), which indicates clearly the preferential transfer of ^{17}O to CO_2 . It is interesting to note that in the case of pure dissociation of ozone, the left-over ozone and product oxygen compositions lie along the same line in the three isotope plot i.e. they follow the same slope (due to mass balance), whereas in the presence of CO_2 the oxygen points deviate and plot along a line of higher slope due to depletion in ^{17}O which end up in CO_2 . This provides a supportive evidence for the preferential transfer of ^{17}O from ozone pool to CO_2 pool. The slope (0.63) in left-over ozone has been explained in Chapter III, § 3.2.4 (also see Chakraborty and Bhattacharya, 2002) arising out of a combination of two effects: pure photo-dissociation of ozone (leading to a slope of unity) and $\text{O}(^1\text{D})$ reaction with ozone (leading to a slope of 0.5).

4.4.5 Results of Set II Experiments: Connection to the Stratosphere

The data from the set II experiments also reflect the same ^{17}O preference over ^{18}O during isotopic exchange. In this set, nine identical samples of CO_2 (100 μmole in size and having same isotopic composition) are made to exchange with nine different ozone samples having widely different isotopic composition but mutually connected along a line of slope 0.63. It is seen that the enrichment transferred to CO_2 reflects that in the

corresponding ozone. If the ozone is more enriched so is the corresponding CO_2 . Interestingly, all the CO_2 points (Figure 4.3) lie along a line of slope 1.94 with corresponding ozone points along a line of slope 0.63. These results cannot be directly compared with those of sets Ia, Ib and Ic, since it demonstrates a different experimental feature. While data from sets Ia, Ib and Ic show the time variation of enrichment with two fixed end members, set II data show the effect in enrichment with a fixed CO_2 end member and variable ozone composition.

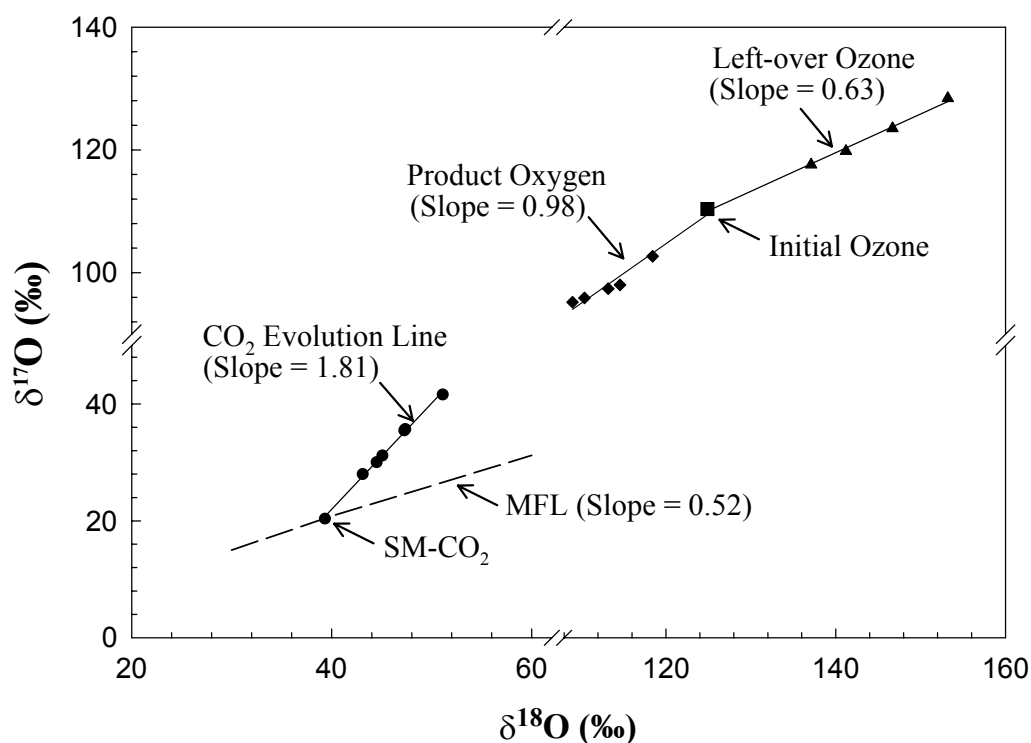


Figure 4.6. A comprehensive three-isotope plot for set I experiment showing the interrelation among the compositions of CO_2 , O_3 and product O_2 . The left-over ozone and the product oxygen follow two different slopes 0.63 and 0.98 respectively (with respect to initial ozone composition), in contrast to the case of simple dissociation of ozone when the left-over ozone and product oxygen follow the same slope of 0.63. This demonstrates a clear depletion of ^{17}O in the product oxygen and preferential transfer of ^{17}O to the CO_2 after exchange with $\text{O}(^1\text{D})$. The error of each data point is comparable to its size.

In the stratosphere, with increasing altitude, oxygen isotopic enrichment in both CO_2 and ozone increases progressively (Lämmerzahl et al., 2002). Interestingly, the enrichment pattern has slope values of 1.71 and 0.62 respectively close to the pattern found in set II data and also in set Ia results. Though the initial CO_2 composition ($\delta^{17}\text{O} = 8.98$ ‰ and $\delta^{18}\text{O} = 17.28$ ‰) and the variation in initial ozone composition (124.9 to 205.7 ‰, i.e. about 80 ‰ in $\delta^{18}\text{O}$) in the laboratory experiment is not representative of

the stratospheric values (the isotopic composition of stratospheric ozone varies only by about 30 ‰ in $\delta^{18}\text{O}$), the slope values observed in these experiments are quite similar to that of stratospheric values (compare stratospheric values with the slopes shown in Figures 4.3 and 4.6 for the laboratory results for set II and Ia respectively). This establishes an invariant isotopic relationship between these two interacting oxygen reservoirs (ozone and CO_2). The stratospheric situation can be envisaged as a combination of the effects arising out of the two types of experiments – one dealing with the time variation and the other dealing with the enrichment variation.

Though the oxygen isotopic composition of CO_2 used in set Ia ($\delta^{17}\text{O} = 20.35$ and $\delta^{18}\text{O} = 39.33$ ‰) is heavier compared to that used in set II ($\delta^{17}\text{O} = 8.98$ and $\delta^{18}\text{O} = 17.28$ ‰), the observed slope value of set Ia (1.81) is lower compared to set II (1.94). However, the initial ozone composition of set II (varied from 124.9 to 205.7 ‰ in $\delta^{18}\text{O}$, Table 4.4) is heavier than that of set Ia ($\delta^{18}\text{O} = 124.9$ ‰, Table 4.3). Therefore, the noticeable point from the combined result of these two sets of experiments is that the slopes in final CO_2 increases with the increase in the initial ozone compositions. In the lower stratosphere the observed variation in isotopic composition of ozone is about 95 to 135 ‰ (in $\delta^{18}\text{O}$ with respect to SMOW) (Mauersberger et al., 2001), which is lower compared to that used in sets Ia and II. Hence, with this lower ozone composition, the lower stratospheric slope (1.71) can be reproduced with SM- CO_2 (equivalent to tropospheric CO_2). More discussion about this issue will be presented in Chapter V.

4.4.6 Preferential ^{17}O Transfer to CO_2

The following scenario is envisaged to explain the observed anomalous ^{17}O enrichment in CO_2 during exchange with $\text{O}(^1\text{D})$. The UV photolysis of the $\text{CO}_2 - \text{O}_3$ mixture for certain duration of time produces $\text{O}(^1\text{D})$ continuously. As the quantum yield of O_3 photo-dissociation (at < 315 nm) is unity (Matsumi et al., 2002), every photon, when absorbed, leads to one $\text{O}(^1\text{D})$ atom and one O_2 molecule. As $\text{O}(^1\text{D})$ is a very reactive species it quenches quickly to $\text{O}(^3\text{P})$ soon after its formation by interaction with product O_2 and CO_2 with high rate coefficients ($4.0 \times 10^{-11} \text{ cm}^3 \text{ s}^{-1}$ and $1.1 \times 10^{-10} \text{ cm}^3 \text{ s}^{-1}$ respectively). Therefore, the CO_2 molecules continuously interact with newly formed $\text{O}(^1\text{D})$ atoms forming CO_3^* complexes, which dissociate to CO_2 and $\text{O}(^3\text{P})$ within its short lifetime ($\sim 10^{-11}$ s). It implies that a fraction of the CO_2 molecules in the system are continuously modified by this process and the total CO_2 is a mixture of the CO_2

molecules which interacted with $\text{O}(^1\text{D})$ and those which did not. During the above mentioned processes, the oxygen isotopic composition of the final CO_2 is determined by that of $\text{O}(^1\text{D})$ and fractionation associated with quenching of $\text{O}(^1\text{D})$ by CO_2 through formation and dissociation of CO_3^* .

The reason for ^{17}O selectivity in CO_2 during quenching via CO_3^* formation/dissociation is not clear but can be speculated based on a few previous studies (Zahr et al., 1975; Harding et al., 1988; Bhattacharya et al., 2000). It is known that the quenching of $\text{O}(^1\text{D})$ by di and tri-atomic molecules such as N_2 , O_2 , CO and CO_2 is extremely efficient. Collision of these molecules with $\text{O}(^1\text{D})$ excites sufficient rotation and vibration in them on a strongly attractive singlet potential energy surface through formation of a collision complex. 1.97 eV energy of the $\text{O}(^1\text{D})$ atom is transferred to the complex molecule by this process and it is converted to $\text{O}(^3\text{P})$ on a dissociating triplet surface. The crossing for singlet to triplet surface is mediated by spin-orbit coupling which is normally weak. But in case of a collision complex with small but finite life-time the crossing point is traversed many times leading to sizeable quenching cross-section. For the present case, *ab initio* calculations (Froese and Goddard, 1993) predict existence of a low-lying bound region of the singlet potential energy surface (corresponding to $\text{O}(^1\text{D}) + \text{CO}_2$ collision), where the CO_3^* formation takes place. In this region, an intersystem crossing to the triplet surface may occur to form the $\text{O}(^3\text{P}) + \text{CO}_2$ as dissociation products. Since the vibrational frequencies of the isotopomers of CO_2 are different, it is possible to imagine that a ^{17}O containing CO_2 molecule has a favorable disposition in the region of cross-over due to a combination of rotational and vibrational energies accounting for major part of the 1.97 eV energy of the $\text{O}(^1\text{D})$. In effect, this will result in slightly more rapid quenching of a ^{17}O containing CO_3^* when the ^{17}O goes to the CO_2 molecule in a process mimicking resonant absorption. A schematic diagram showing such a singlet-triplet transition with matching of vibrational levels is given in Figure 4.7 for illustration. A similar resonant process of ^{17}O enrichment in product oxygen in dissociation of CO_2 by UV has been recently found by Bhattacharya et al. (2000). It is to be noted that such a near-resonance effect was also postulated by Harding et al. (1988) to explain the unusual efficiency of CO in quenching of $\text{O}(^1\text{D})$. The 1.97 eV energy of $\text{O}(^1\text{D})$ matches closely the energy required to excite $\nu = 7, 8$ vibrations of CO molecule through spin-orbit induced surface crossing of a long-lived complex CO_2^* from $^1\text{B}_2$ state to $^3\text{B}_2$ state.

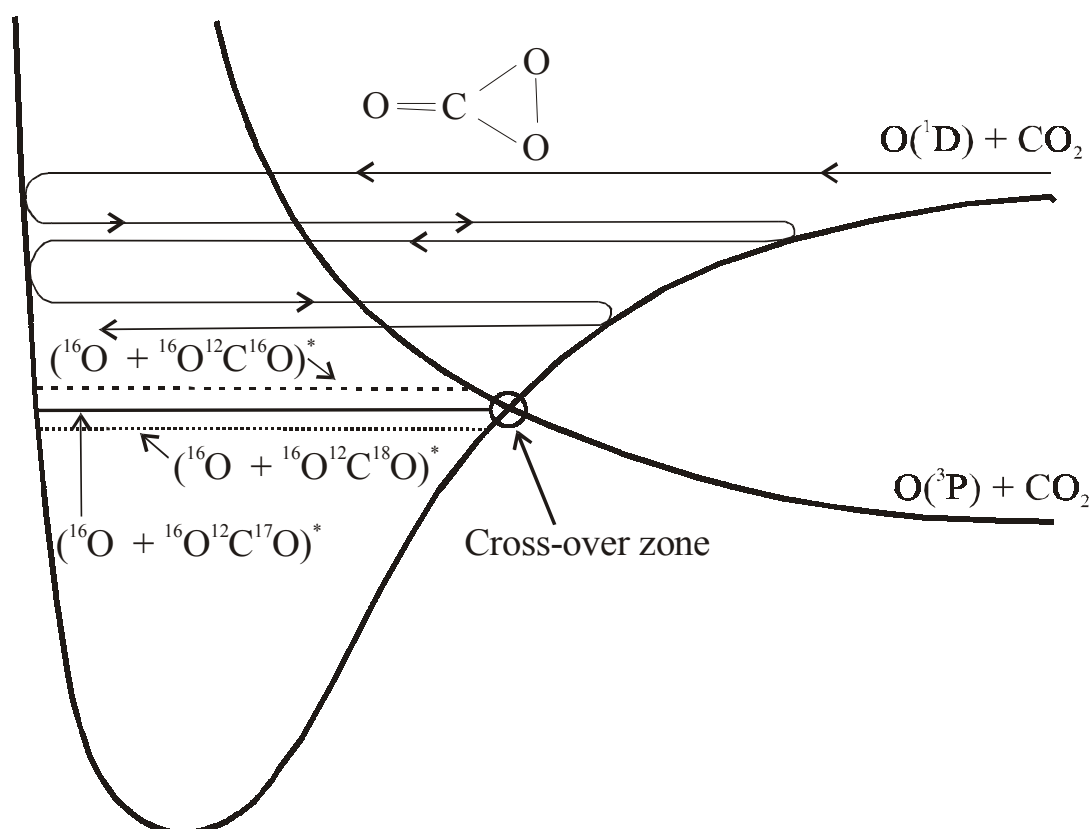


Figure 4.7. A schematic of the lowest singlet and a typical triplet potential energy curves for $\text{CO}_2 - \text{O}(^1\text{D})$ system. The arrow depicts a collision of $\text{O}(^1\text{D})$ and CO_2 which results in rotational /vibrational excitation of the transient molecule (occurring predominantly at the inner classical turning point) to form a collision complex. It is proposed that a better matching of rovibrational levels of ^{17}O containing CO_2 with the cross-over zone favors its formation in quenching of $\text{O}(^1\text{D})$.

It is also possible that coupling by nuclear spin of ^{17}O plays a role. Among the three isotopes of oxygen, only ^{17}O has nuclear spin (5/2). Since the singlet-triplet transition is spin-forbidden it can only be affected by a spin-orbit interaction and an addition to the total perturbation from the nuclear spin of ^{17}O may increase the quenching probability.

4.4.7 A Simple Box Model Calculation

Following the reaction sequence outlined above one can empirically derive the magnitude of the extra fractionation in ^{17}O during CO_3^* formation/dissociation step from the experimental data. Keeping in mind the production of $\text{O}(^1\text{D})$ during the photolysis of $\text{O}_3 - \text{CO}_2$ mixture, an $\text{O}(^1\text{D})$ generator is assumed which continuously supplies $\text{O}(^1\text{D})$ into the system. The entire process (shown schematically in Figure 4.8) is thought to be

consisting of a large number of cycles. In each cycle, a small part of CO_2 interacts with $\text{O}(^1\text{D})$ and forms CO_3^* complex. The isotopically modified CO_2 generated from CO_3^* decomposition mixes up with the rest of the CO_2 . In this process the oxygen isotopic composition of the total CO_2 changes. After a large number of similar cycles the oxygen isotopic composition of final CO_2 will be markedly different from that of the initial composition.

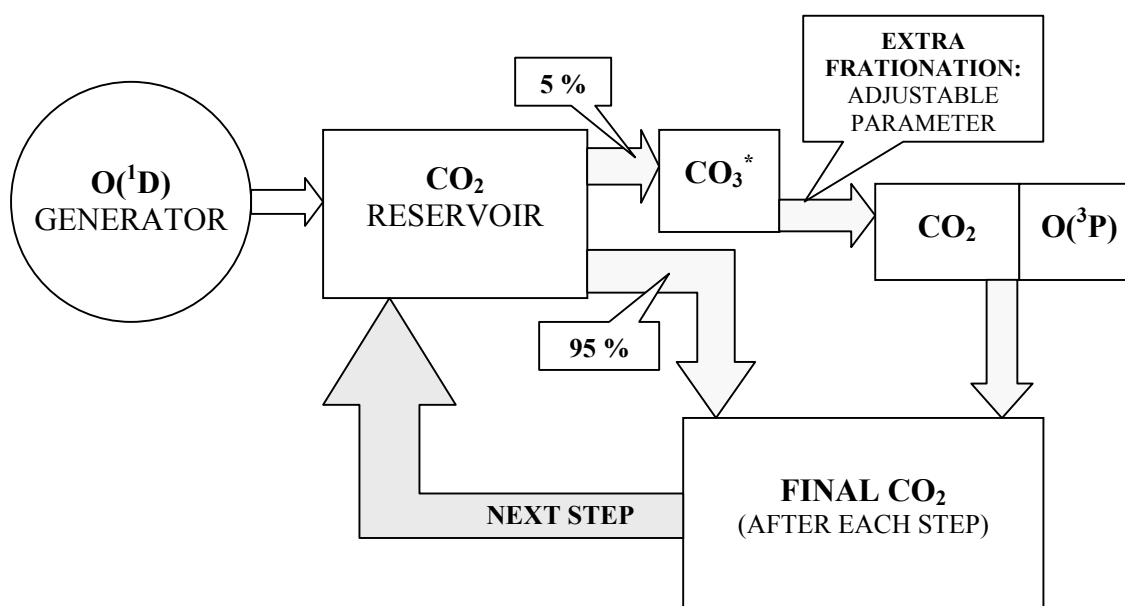


Figure 4.8. A schematic pathway of the box model showing a single cycle. In reality, this cycle operates large number of times to change the isotopic composition of the final CO_2 . No reservoir of $\text{O}(^1\text{D})$ was assumed, rather a constant source of $\text{O}(^1\text{D})$ was considered. In each cycle 5 % of reservoir CO_2 interacts with $\text{O}(^1\text{D})$ and mixes up with 95 % un-reacted CO_2 to change the isotopic composition of CO_2 reservoir.

To compute the modified composition of CO_2 in each step, the isotopic composition of CO_3^* was first calculated by two component ($\text{O}(^1\text{D})$ and CO_2) mixing. Next, a mass balance calculation (assuming 95 % original CO_2 and 5 % modified CO_2) yields the composition of the final CO_2 . Since there is no time parameter in the model, 5 % modified CO_2 essentially represents the step size. A free parameter is introduced during CO_3^* formation/decomposition step through which an extra fractionation from CO_3^* decay can be added. The isotopic composition of $\text{O}(^1\text{D})$ is considered to be equal to that of asymmetric ozone modified for collision as mentioned before ($\delta^{17}\text{O} = 138.1 \text{ ‰}$ and $\delta^{18}\text{O} = 127.6 \text{ ‰}$) and the CO_2 composition is assumed to be the same as modified SM- CO_2 (applicable to set Ia experiment).

The model is run with the above parameters and compositions. It is seen that to generate a slope of 1.81 (for set Ia experiment) an extra fractionation of 16.5 ‰ in ^{17}O needs to be introduced (through the free parameter mentioned above). Interestingly, with the same amount of extra fractionation in ^{17}O , the model predicts slopes of values 1.46 and 1.36 when the initial CO_2 composition is changed to that of modified SP- CO_2 and modified SL- CO_2 respectively. These two slopes compare well (within errors) with the values (i.e. 1.52 and 1.29) obtained in experiments of set Ib and set Ic respectively. The consistency of the extra enrichment in $^{17}\text{O}/^{16}\text{O}$ ratio of the final CO_2 between the three sets is reassuring, since it shows that a fixed amount of fractionation is associated with CO_3^* formation / decomposition process, which favors ^{17}O more than ^{18}O in the final product.

4.5 CONCLUSION

The transfer of “heaviness” from the ozone pool to the CO_2 pool in UV-induced exchange reaction is not by simple mixing of CO_2 with $\text{O}(^1\text{D})$ but has a component due to fractionation from intermediate CO_3^* , which favors ^{17}O transfer relative to ^{18}O . Present experiments were designed to provide further insight in this transfer mechanism and explain the data pertaining to the stratosphere. The evolution of the exchanged- CO_2 was examined by taking three different initial CO_2 compositions and a fixed ozone composition. The trend in final CO_2 was also investigated using a fixed CO_2 composition and varying initial ozone composition. Though the experimental set up does not exactly correspond to the stratospheric condition, the results bring out the essential feature of the stratospheric process governing the oxygen isotopic distribution among ozone and CO_2 reservoir in stratosphere. Analysis of the data suggests that the processes associated with formation/dissociation of the collision complex CO_3^* contribute an extra enrichment in ^{17}O to the product CO_2 . We postulate that a process similar to resonant absorption takes place during the quenching of $\text{O}(^1\text{D})$ by CO_2 such that ^{17}O containing isotopomers of CO_2 are favored during dissociation of the CO_3^* complex which takes place through transition from a singlet to triplet state.